J. Braz. Chem. Soc., Vol. 10, No. 6, 497-504, 1999.
Printed in Brazil.

0103 – 5053 $6.00 + 0.00

Article

PS-HEMA Latex Fractionation by Sedimentation and Colloidal Crystallization

André H. Cardoso, Carlos A.P. Leite, and Fernando Galembeck*

Instituto de Química, Universidade Estadual de Campinas,

130803-970 Campinas - SP, Brazil

Látex de poli(estireno-co-hidroxiacrilato de metila) separa-se em três camadas visualmente distinguíveis, das quais a inferior é opalescente e contém cristais coloidais. Alíquotas do látex foram coletadas em diferentes alturas, e as partículas foram caracterizadas, por espalhamento de luz dinâmico, microeletroforese, IV e microscopia eletrônica analítica. A fração inferior contém a maior parte do polímero, sendo formada por partículas de dimensões e composição química uniformes. As partículas coletadas das duas outras frações são diferentes das que formam os cristais coloidais, em praticamente todos os aspectos. A secagem da fração opalescente produz macrocristais de alta qualidade, com baixa frequência de defeitos, mostrando que a homogeneidade química das partículas é um fator importante, na sua auto-organização.

A poly(styrene-co-hydroxyethylmethacrylate) latex underwent sedimentation under gravity followed by an spontaneous and extensive colloidal crystallization. It was then fractionated in three visually distinguishable layers. Latex aliquots layers were sampled at different heigths and the particles were characterized by PCS, microelectrophoresis, infrared spectra and analytical electron microscopy. The major fraction was opalescent and contained the colloidal crystals settled in the bottom of the liquid. Two other latex fractions were obtained, which differed in their chemical compositions, particle sizes and topochemical features from the self-arraying particles. Macrocrystallization of the fractionated latex yielded high quality crystals with a low frequency of defects, which confirms that particle chemical homogeneity is an important factor for particle self-arraying.

Keywords: *latex fractionation, colloidal crystallization, latex sedimentation, core-and-shell latex, macrocrystal, latex*

Introduction

Self-organized latex particle arrays[1,2], either (dry) macrocrystals or (liquid) colloidal crystals, are often observed in latexes, and they have attracted the attention of many researchers. Many devices have been proposed to help building high quality macrocrystals, but the success rate is still low[3-7] considering both the number of macrocrystalline domains obtained and the extent of correlated crystalline planes. On the other hand, many colloidal crystal-forming systems are known, and their equilibria with the colloidal "gas" phase[8] have been studied but the formation of high quality colloidal crystals is still an exception rather than the rule. Practical applications of these structures call for a high degree of control over the processibility as well as the structure and composition of the latex[9].

*e-mail: fernagal@iqm.unicamp.br

Two conditions are usually fulfilled, in successful attempts of latex colloidal crystallization: the particle diameters are monodisperse and the ionic strength of the initial dispersion liquid is very low[10-11]. The importance of hydrophilic particle surfaces and capillary adhesion in the formation of dry macrocrystals is well acknowledged, following the work of Denkov, Nagayama *et al.*[12], Distler and Koenig[13], Whitesides and collab.[3]. In a paper on disorder-to-order in settling suspensions of colloidal silica, Davis *et al.*[7] observed that ordered particle arrays were obtained at higher solid volume fractions ($\phi > 0.5$), but only when the rate of particle sedimentation is lower than the rate of particle crystallization.

We have recently examined in detail the case of poly(styrene-co-hydroxyethylmethacrylate) latex, in

which the particle polidispersity as well as the presence of salt in the initial dispersion does not preclude macrocrystallization[14]. In another recent work, we have obtained microchemical information on this latex, by energy-loss imaging (ESI)[15]. This showed that negative charges are distributed throughout the dry latex particles, while the positive charges make a particle shell in the dry particles, thus imparting to each particle a multipolar charge distribution which is relevant for particle-particle interaction and self-arraying. We confirmed that these particles are dipoles or multipoles, by observing backscattered-electron images in a field-emission electron microscope as well as by showing that the charge-bearing groups in the particles are asymmetrically distributed[16].

Latex particle chemical heterogeneity is now well established[17,18], and techniques are available to observe differences in the chemical composition from one to another particle in a population, as well as for the microchemical characterization of domains within individual particles.

In this work, we report on the fractionation of PS-HEMA latex, and we show that this actually leads to high-quality macrocrystal formation.

Experimental

Latex preparation and characterization

The latex was prepared[14] by batch surfactant-free emulsion copolymerization of styrene (S) and hydroxyethyl methacrylate (HEMA) following procedures similar to those developed by Okubo[19] and Suzawa[20]. The amounts of reagents used are as follows: water 210.2 g, styrene 31.2 g, 2-hydroxyethyl methacrylate 4.5 g, potassium persulfate 0.1086 g.

The polymerization was carried out in a 500 mL glass kettle reactor fitted with condenser, thermometer, glass paddle-type stirrer and a gas inlet providing a constant flow of nitrogen gas. The kettle was kept at the required constant temperature (±2 °C) using a thermostated water bath. The reaction vessel was loaded with water and the monomers, and heated to 70 °C. After 30 min of N_2 purging and stirring the system, the initiator potassium persulfate dissolved in 4.5 cm^3 of water was added to the reaction mixture. The polymerization reaction was carried out at 70 °C for 10 h under constant 300-350 rpm stirring. The product was filtered with a 200 mesh steel sieve, to remove coagulated latex. In order to remove unreacted monomer, oxidation products and unwanted electrolyte, the resulting latex was dialyzed against water with daily changes over a two-month period. The dialysate conductivity reached 2 μS/cm, and remained unchanged for 48 h. The dialysis tubing (a visking membrane from Sigma) was boiled in several quantities of distilled water, prior to use.

After dialysis, part of the latex sample was lyophilized using a bench-top glass apparatus, to recover the solid polymer for spectral characterization. The remainder of the sample was dispersed in water, as required for reaching the desired concentration. Monomer conversion was 94.4%, as determined gravimetrically right after the reaction[14].

Transmission electron microscopy and elemental spectroscopy imaging

Brightfield pictures and the elemental distribution within latex particles were obtained using a Carl Zeiss CEM 902 transmission electron microscope, equipped with a Castaing-Henry-Ottensmeyer energy filter spectrometer within the column. When the electron beam passes through the sample, interaction with electrons of different elements results in characteristic energy losses. A prism-mirror system deflects electrons with different energies to different angles so that only electrons with a well defined energy are selected. If elastic electrons only are chosen ($\Delta E = 0$ eV) a transmission image with reduced chromatic aberration is obtained. When monochromatic inelastically scattered electrons are selected, electron spectroscopic images (ESI) are formed, in which contrast is dependent on the local concentration fluctuations of a particular chosen element. Clear areas correspond to element-rich domains.

For individual latex particle examination, one drop of the latex dispersion (1% solids content) was deposited on carbon-coated parlodion films supported in 400 mesh copper grids (Ted Pella). To make sure that the whole particles were not excessively thick, they were first observed using $\Delta E = 0$ eV electrons, then observed again at $\Delta E = 20$-50 eV. Image contrast inversion was always obtained, showing that a significant number of electrons were transmitted throughout the particles[21]. This observation is understood, considering that the 80 keV electrons mean free path within these latex particles is greater than 160 nm for elastic scattering[22], and is estimated as many hundreds of nanometers, for inelastic scattering.

Elemental images were observed for the relevant elements found in this sample, using monochromatic electrons corresponding to the carbon K-edge, oxygen K-edge, sulfur L-edge and potassium L-edge with an energy-selecting slit of 15 eV. The energy-selecting slit was set at 278 ± 6 eV for C, 532 ± 6 eV for O, 165 ± 6 eV for S and 292 ± 6 eV for K. The images were recorded by a MTI-Dage SIT-66 camera and digitized (512 x 480 pixels, 8 bits) by an IBAS image analyzer software from Kontron running on an IBM PC-AT compatible microcomputer. The three-window

technique was used to perform the background subtraction, for each elemental image[23].

Image processing was performed in an IBM PC microcomputer using the Image-Pro Plus 3.0 image analyzer program (Media Cybernetics).

FESEM images

Secondary electron images were obtained in an ultra high resolution "semi-in-lens" JEOL JSM-6340F field emission scanning electron microscope, operating at 15 kV, which corresponds to a 1.2 nm nominal resolution. The films were placed on a metal stub and sputter coated with carbon prior to examination.

Infrared spectra

Infrared spectra were obtained from polymer films cast on NaCl windows. The latex fractions were centrifuged, the latex was dried and dissolved in toluene, to obtain the casting solutions.

Results

Latex sedimentation under gravity

Soon after its synthesis, *ca.* 200 mL of the latex dispersion were stored in a 250-mL glass vial with a screw-cap (*ca.* 63 mm i.d.; initial liquid height was 115 mm). After 5 months storage, an intensely opalescent, 15-mm high layer was observed at the bottom of the container. Visual observation at any given angle showed the existence of domains, presenting iridescent colors extending for a few centimeters within this bottom layer, which changed with the angle of observation. This proves that there was a high degree of ordering in this layer, characterized by macroscopic colloidal crystals. Many bright, millimeter-sized spots of different colors were also observed, evidencing the coexistence of colloidal polycrystals. There is a well-defined interface between this crystalline layer and an opaque milky layer above it, and another upper, translucent layer, 1-mm thick just beneath the latex surface.

Three aliquots were carefully collected with syringes fitted with long glass tips, to avoid cross-contamination. The fractions were drawn: i) from the opalescent layer, ii) from the milky layer, 30 mm above the bottom and iii) 50 mm above the bottom.

Properties of the particles in the separated latex fractions

The solids contents in the three layers were determined, as well the particle sizes and zeta potentials. The results are in Table 1.

Transmission brightfield micrographs are in Fig. 1. The two upper fractions contain large numbers of small (< 200 nm) particles, which are not seen in the lower fraction. There are also important differences among the larger particles in the three fractions: in the lower fraction, the particles in the microscope grid are well separated, and they do not show any strong trend towards coalescence, as evidenced by necking. On the other hand, larger particles in the upper fractions coalesce with the smaller particles and with larger particles (not shown), as well. This demonstrates significant differences in larger particle surface properties, even though their diameters are very close, in the different fractions.

The smaller particles are very different from the larger ones, also considering their smooth surfaces, departure from spherical shapes and their easy coalescence as evidenced by the pronounced neck formation.

Consequently, the coexistence of ordered and disordered material within this latex is not the result of an order-disorder phase equilibrium, but instead it is the result of latex particle fractionation.

Electron spectroscopy imaging of the disordered fractions

Figures 2-5 present micrographs and elemental (C, O, S and K) distribution maps, for particles in the three latex aliquots. In the bottom fraction, the particles are all similar, in the different maps. This demonstrates a rather uniform overall chemical composition, for these particles. On the other hand, the opposite is observed in the intermediate fraction, particularly among the smaller particles. Some specific observations are the following:

i) Some small particles appear brighter than others in the top fraction sulfur map (Fig. 4), but these same particles are not distinguished in the carbon map (Fig. 2). Consequently, these particles have an above-than-average sulfur/carbon atom ratio, probably associated with a lower MW of the polymer chains.

Table 1. Concentration, particle effective diameters and zeta potentials for the three latex fractions.

Latex fraction	Supernatant	Intermediate	Bottom layer (opalescent)
Concentration (w%)	0.2	0.1	28
Effective diameter (nm)	159 ± 7	189 ± 2	423 ± 5
Zeta potential (mV)	-36 ± 4	-42 ± 5	-53 ± 1

ii) The oxygen map in Fig. 3 also shows some darker particles, which are nevertheless very clear in the carbon and potassium maps. The conclusion is the existence of a significant variation in the O/C ratio, and the existence of styrene-richer (and acrylate-poorer) small particles.

iii) Even in the very uniform particles in the bottom fraction, a few brighter points are observed (*e.g.*, in the particle to the right, *ca.* 5 o'clock in Fig. 3c), showing domains in which C content is higher than average.

iv) In the top fraction, potassium is distributed rather uniformly (Fig. 5) throughout the coalesced particles. In the intermediate fraction this ion tends to concentrate at the outer shell of either larger or smaller particles, and in the

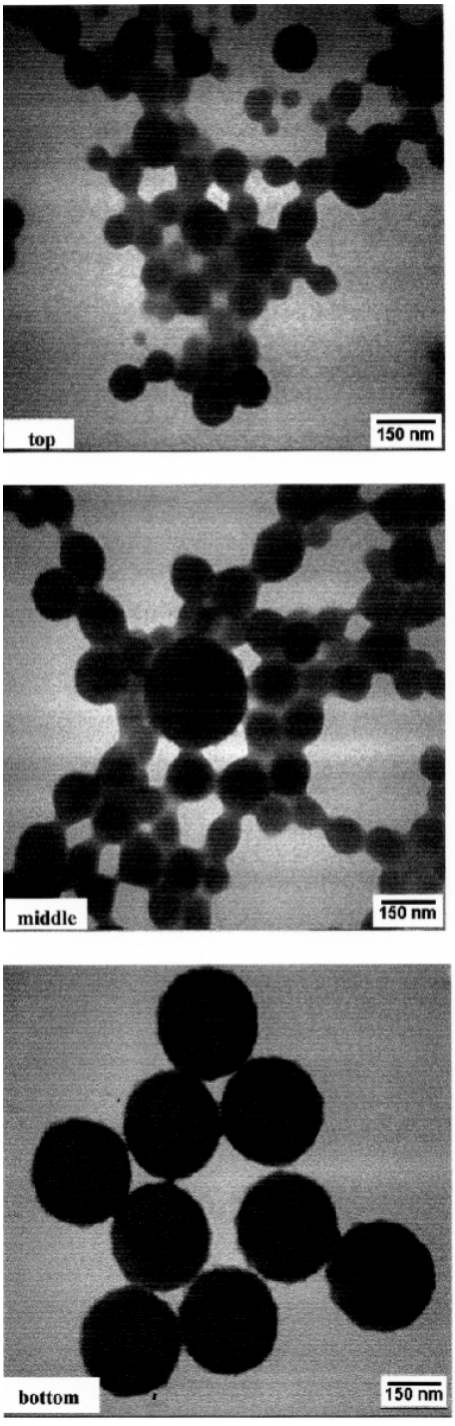

Figure 1. Brightfield transmission electron micrographs of particles from the three fractions collected from the latex.

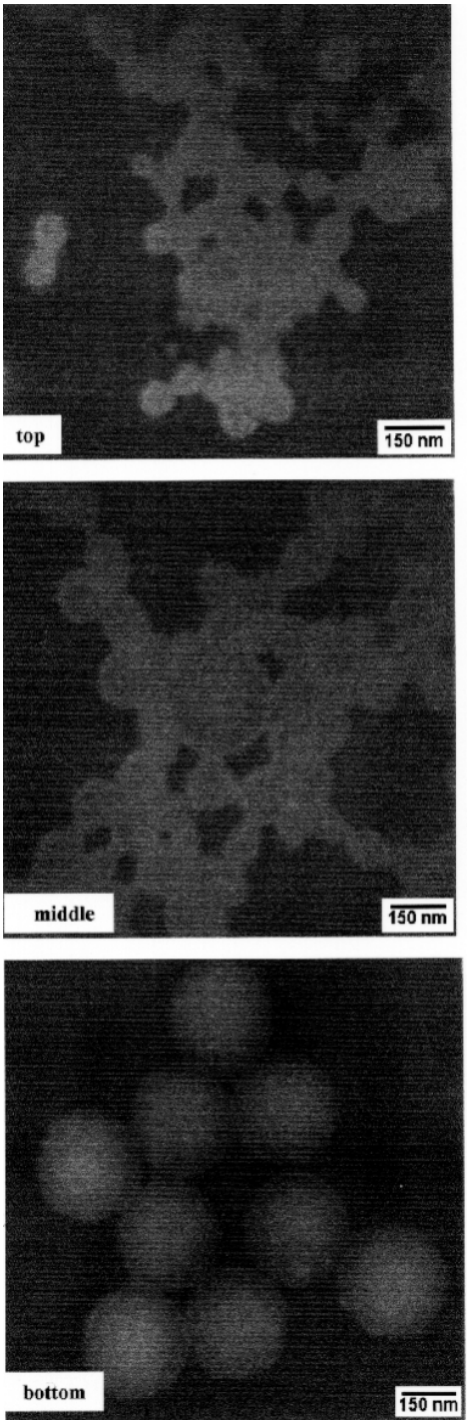

Figure 2. C elemental distribution maps of the upper, medium and bottom fractions collected from the latex.

lower fraction potassium concentration at the particle surface is very marked.

Infrared spectra

Infrared spectra for films obtained for the three aliquots are in Fig. 6. The spectra for the two upper fractions are rather similar, but they show large differences with the bottom fraction, particularly in the 1300-1050 cm^{-1} range. The spectrum of the bottom fraction in this range corresponds closely to the sum of the homopolymers spectra. Consequently, these particles are predominantly formed by block copolymer chains, or by a mixture of homopolymers.

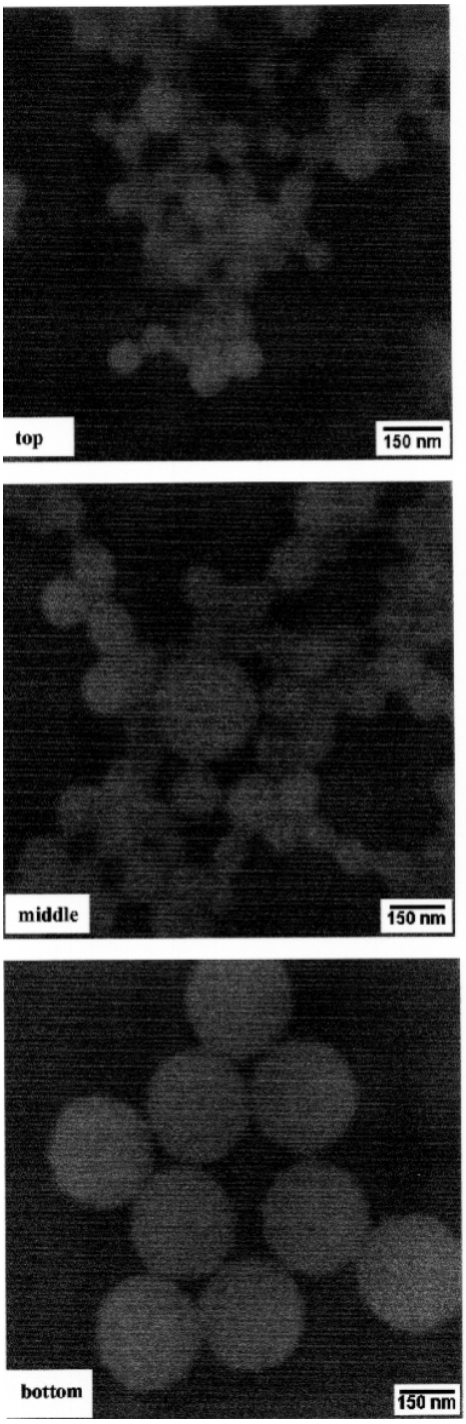

Figure 3. O elemental distribution maps of the upper, medium and bottom fractions collected from the latex.

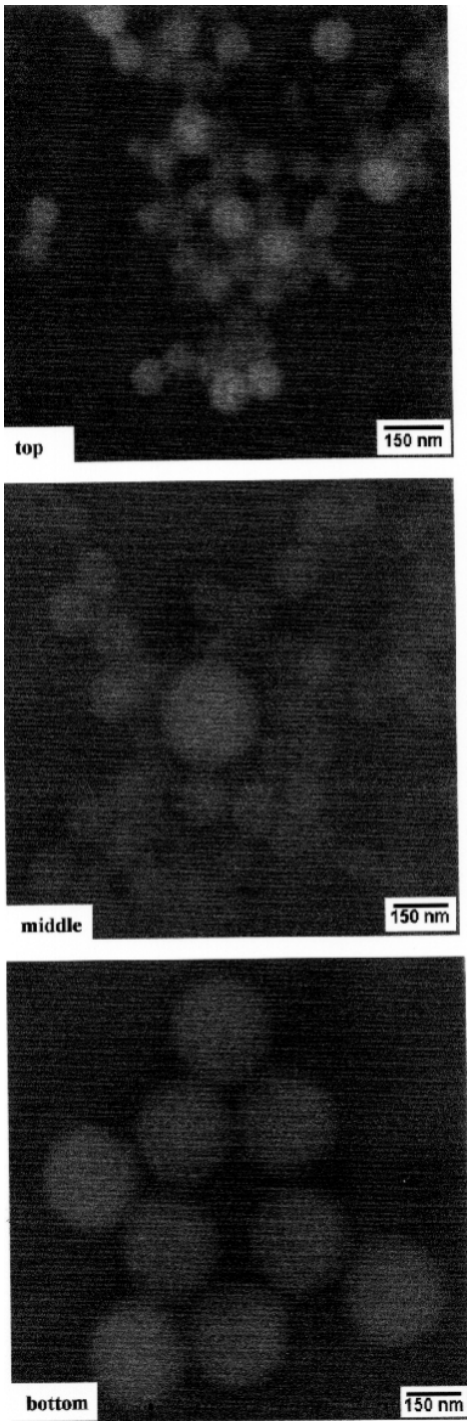

Figure 4. S elemental distribution maps of the upper, medium and bottom fractions collected from the latex.

The poor resolution of the bands in this same region, for the two upper fractions, is an evidence that the acrylic mers are interspersed with styrene, forming random copolymer chains[24].

The ratios between the absorbances at 1727 (assigned to C=O acrylic groups) and 700 (from out-of-plane aromatic ring deformation) cm^{-1} in the three fractions are respectively 11.1, 4.8 and 0.77, while this ratio for the unfractionated latex is 0.83. The particles in the upper fractions are thus much richer in acrylic monomer (which confirms the information from ESI imaging) than the predominating population.

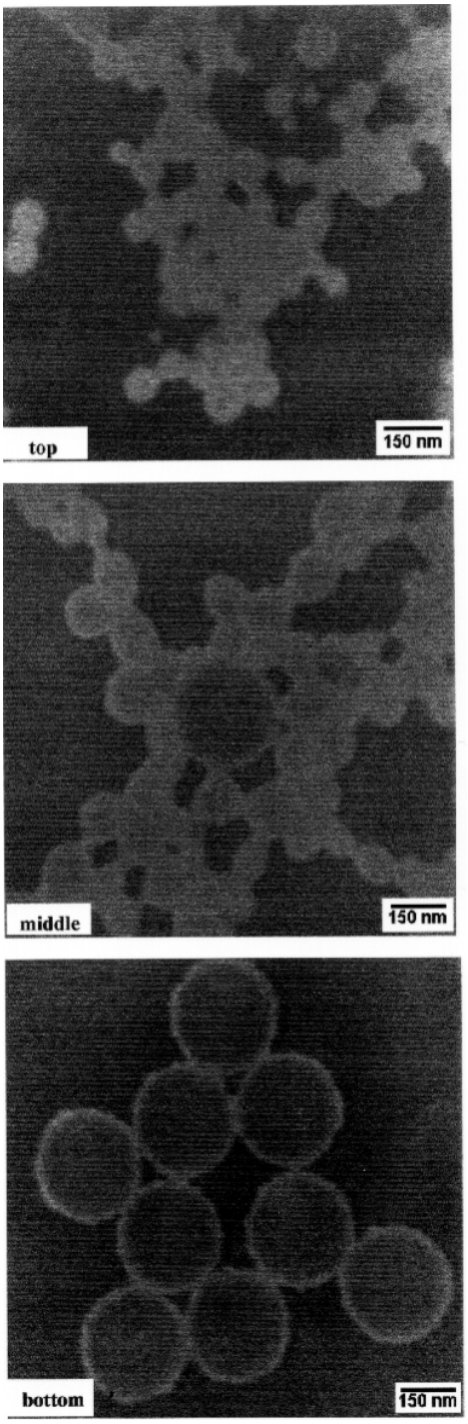

Figure 5. K elemental distribution maps of the upper, medium and bottom fractions collected from the latex.

Scanning electron microscopy

A scanning electron micrograph of a fractured macrocrystal prepared by drying an aliquot of the bottom fraction is presented in Fig. 7. We note the perfection of the particle ordering in this image, which demonstrates the usefulness of particle fractionation, to prepare high-quality macrocrystals.

Discussion

The fractionation of the PS-HEMA latex revealed that even the as-prepared latex is already rather homogeneous. This is probably related to the specific synthesis protocol used in this work; in a previous work, we found significant differences in the degree of heterogeneity of three styrene-butyl methacrylate latexes, depending on the specific synthesis procedure[24].

The lower, opalescent, fraction is by far much more concentrated than the others, and this is probably the main factor for the easy self-arraying of this latex, even prior to fractionation. On the other hand, latex fractionation eliminates particles of many different sizes and chemical compositions, which can only impair crystallization.

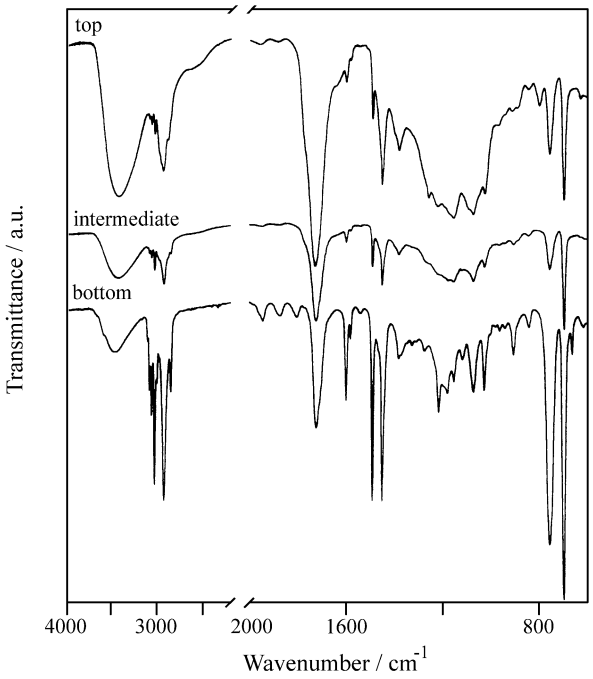

Figure 6. Infrared spectra of films prepared with the three latex fractions.

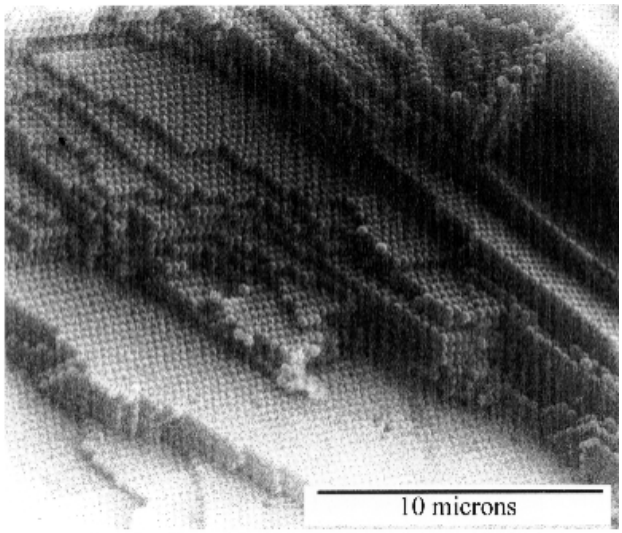

Figure 7. A scanning micrograph of a fractured PS-HEMA macrocrystal. Note the large number of perfectly correlated crystal planes.

The present results show that latex particles undergo an spontaneous sedimentation-driven crystallization, producing a fraction with improved *chemical* uniformity. This fraction has a great ability for colloidal and macrocrystal formation.

In a previous work[16] we have shown that PS-HEMA latex particles are dipoles (or multipoles), and we proposed that this feature is relevant for self-arraying. In the present paper we have described the extensive spontaneous formation of colloidal crystals at rather low (28%) volume fraction, in an undialyzed sample, and we suggest that the polar nature of the particles contributes to this behavior.

The present findings give us an explanation for the difficulties in observing and reproducing self-arrayed latex structures, even in size-monodisperse latex: this is probably due to a large heterogeneity of particle chemical compositions, which poses difficulties for the encounters of identical particles, with good associating characteristics.

On the other hand, we observe that colloidal crystallization is an effective tool for latex purification, which is understood here as the process yielding a highly uniform fraction, concerning size, morphology as well as particle chemical composition.

In the present case this was done just by sedimentation under gravity, but other fractionation techniques (centrifugation in density gradients, osmocentrifugation[25]) are likely to be helpful, as well.

Conclusion

The PS-HEMA latex sediments under gravity and it undergoes spontaneous fractional colloidal crystallization, yielding a large fraction of chemically and morphologically uniform particles. Minor fractions contain particles with large chemical differences, in a range of diameters. The predominance of chemically uniform particles in the as-prepared latex explains the unusually easy macrocrystallization of this latex.

Acknowledgments

FG acknowledges the support of Fapesp, Pronex/Finep/MCT and CNPq. During this work, AHC was a Capes pre-doctoral fellow.

References

1. Alfrey Jr., T.; Bradford, E.B.; Vanderhoff, J.W.; Oster, G. *J. Opt. Soc. Am.* **1954**, *44*, 603.
2. Hachisu, S.; Kobayashi, Y.; Kose, A.J. *J. Colloid Interface Sci.* **1973**, *42*, 342.
3. Kim, E.; Xia, Y.; Whitesides, G. *Adv. Mater.* **1996**, *8*, 245.
4. Michelleto, R.; Fukuda, H.; Ohtsu, M. *Langmuir* **1995**, *11*, 3333.
5. Trau, M.; Saville, D.A.; Aksay, I.A. *Science* **1996**, *272*, 706.
6. Burmeister, F.; Schäfle, C.; Matthes, T.; Böhmisch, M.; Boneberg, J.; Leiderer, P. *Langmuir* **1997**, *13*, 2983.
7. Davis, K.E.; Russel, W.B.; Glantschnig, W.J. *Science* **1989**, *245*, 507.
8. Böhmer, M. *Langmuir* **1996**, *12*, 5747.
9. Meier, W. *Curr. Op. Colloid Interface Sci.* **1999**, *4*, 6.
10. Joanicot, M.; Wong, K.; Maquet, J.; Chevalier, Y.; Pichot, C.; Graillat, C.; Lindner, P.L.; Rios, Cabane B. *Progr. Colloid Polym. Sci.* **1990**, *81*, 175.
11. Keddie, J.L. *Materials Science and Engineering* **1997**, *R21*, 101.
12. Denkov, N.D.; Velev, O.D.; Kralchevsky, P.A.; Ivanov, I.B.; Yoshimura H.; Nagayama, K. *Nature* **1993**, *361*, 26.
13. Distler, D.; Kanig, G. *Colloid Polym. Sci.* **1978**, *256*, 1060.
14. Cardoso, A.H.; Leite, C.A.P.; Galembeck, F. *Colloids Surfaces A* **1998**, *144*, 207.
15. Cardoso, A.H.; Leite, C.A.P.; Galembeck, F. *Langmuir* **1998**, *14*, 3187.
16. Cardoso, A.H.; Leite, C.A.P.; Galembeck, F. *Langmuir* **1999**, *15*, 4453.
17. Moita Neto, J.M.; Cardoso, A.H.; Testa, A.P.; Galembeck, F. *Langmuir* **1994**, *10*, 2095.
18. Galembeck, F.; Souza, E.F. In *Polymer Interfaces and Emulsions*, Esumi, K., ed., M. Dekker, New York, p. 119, 1999.

19. Kamei, S.; Okubo, M.; Matsuda, T.; Matsumoto, T. *Colloid Polym. Sci*. **1986**, *264*, 743.
20. Tamai, H.; Fujii, A.; Suzawa, T. *J. Colloid Interface Sci*. **1987**, *116*, 37.
21. We are grateful to Dr. W. Probst (LEO-Zeiss Elektronenmikroskopie Gmbh) for this valuable private communication.
22. Newbury, D.E. In "Principles of Analytical Electron Microscopy" Joy, D.C.; Romig Jr., A.D.;Goldstein, J.I., eds., Plenum Press, New York, 1986.
23. Reimer, L.; Zepke, U.; Moesch, J.; Schulze-Hillert, St.; Ross-Messemer, M.; Probst, W.; Weimer, E. "EELS Spectroscopy: A Reference Handbook of Standard Data for Identification and Interpretation of Electron Energy Loss Spectra and for Generation of Electron Spectroscopic Images" Carl Zeiss, Oberkochen, 1992.
24. Cardoso, A.H.;.Moita Neto, J.M; Leite, C.A.P.; Galembeck, F. *Colloid Polymer Sci.* **1997**, *275*, 244.
25. Galembeck, F.; Robilotta, P.R.; Pinheiro, E.A.; Joekes, I.; Bernardes, N. *J. Phys. Chem.* **1980**, *84*, 112.

Received: August 6, 1999

FAPESP helped in meeting the publication costs of this article